Can we predict short term extreme conditions from 10-minute data only?

Paper

Hannesdóttir, Ásta; Larsen, Gunner Chr.; Svensson, Elin

Published in:
Journal of Physics: Conference Series

Link to article, DOI:
10.1088/1742-6596/1452/1/012025

Publication date:
2020

Document Version
Publisher's PDF, also known as Version of record

Can we predict short term extreme conditions from 10-minute data only?

Can we predict short term extreme conditions from 10-minute data only?

Ásta Hannesdóttir, Gunner Chr. Larsen and Elin Svensson

Technical University of Denmark, Department of Wind Energy, Frederiksborgvej 399, 4000 Roskilde Denmark

E-mail: astah@dtu.dk

Abstract. In this study we compare 50-year return values of extreme estimates from a model to values estimated from data analysis. The outputs present a suite of extreme wind load conditions relevant for wind turbine design. The input parameters for the model consist of only statistical wind data, rather than high-frequency measurements that are less available. The model generally predicts lower extreme values than prescribed in the IEC wind turbine safety standard and is therefore of great interest to wind turbine manufacturers. This is the first time a systematic validation of the full suite of extreme models is performed in the whole wind speed range. The accuracy of the model predictions is estimated using a comprehensive data set from a complex terrain site. It is found that the mean absolute percentage error between the data analysis and the model outputs lies within the range of 8.1% - 65.8%.

1. Introduction

The model of Larsen[1] predicts a set of extreme wind load conditions relevant for wind turbine design. These extreme conditions correspond to four prescribed extreme conditions of the IEC standard for wind turbine safety [2, 3], namely extreme operating gust (EOG), extreme wind shear (EWS), extreme coherent gust with direction change (ECD) and extreme direction change (EDC). Assuming the IEC prescribed Weibull or Rayleigh distribution of mean wind speeds, the advantage of using the Larsen model is that the only required input parameters are the reference turbulence intensity (I_{ref}) and annual-average wind speed (V_{ave}) combined with knowledge of the site-specific terrain type. This model is of great interest to wind turbine manufacturers and others performing site assessment or turbine certification, as it generally predicts lower extremes than those prescribed in the IEC standard. Furthermore, the model parameters may be estimated solely from data consisting of 10-minute average wind speed and standard deviations that often are readily available, thus limiting the need for high-frequency measurements. While the model is based on solid theory of extreme excursions [7, 8] it has not yet been systematically validated against high-frequency measurements, where the extreme wind speed excursions have been estimated as function of wind speed. Only crude preliminary validation has been made on selected parts of the model [5, 6], without wind speed dependence, without rise time considerations, and without proper filtering of the wind speed measurements.

The aim of the current study is to:

- Implement the Larsen model, using site-specific I_{ref} and 10-minute mean wind velocity distribution, while all other assumptions and inputs come from IEC formulations.

- Use site-specific turbulence length scale and updated turbulence intensity considerations for the Larsen model.
- Estimate extreme values corresponding to the EOG, ECD, EDC and EWS directly from measurements.
- Compare the Larsen model predictions with the estimated extreme values.

High-frequency wind measurements from a moderately complex site is used to estimate extreme events. The measurements are low-pass filtered with the same cut-off frequency as used for the parameter estimation of the Larsen model. The joint description of the estimated extreme values and wind speed are extrapolated to 50-year return period contours, by means of the inverse first-order reliability method (IFORM) [11]. We assume the results from the IFORM analysis may be used as a basis to compare with the Larsen model outputs and evaluate whether the model is suitable for site-specific extreme estimates by use of 10-minute wind speed statistics only. The focus of the current study is not only to validate the Larsen model, but also to investigate how good extreme estimates can be achieved with the model based entirely on IEC turbulence assumptions.

2. Site and measurements

The Perdigão 2017 field campaign took place in Vale do Cobrão in central Portugal. The area is characterized as moderately complex and consists of a two-dimensional valley located between two parallel ridges (Figure 1). The terrain is covered by a vegetative canopy with an average height of around 10 m [9]. A wind turbine is located on the southeastern ridge, while the dominant wind direction is perpendicular to the ridges [9]. In the field campaign, the area was monitored by a dense network of instruments, including nine meteorological masts belonging to DTU Wind Energy. The mast locations are shown in Figure 2, where 100 and 60 m masts are marked with red and orange circles, respectively. In this study, wind data from Tower 29 has been used. Tower 29 is located on the northeastern ridge (at a height of approximately 450 m) and is equipped with a Gill WM Pro sonic at 10, 20, 30, 40, 60, 80 and 100 m a.g.l. The sonic measures with a frequency of 18 Hz. The boom directions ranges from 130-138° [10].

Figure 1. The valley between the parallel ridges in Perdigão, looking northwestward.

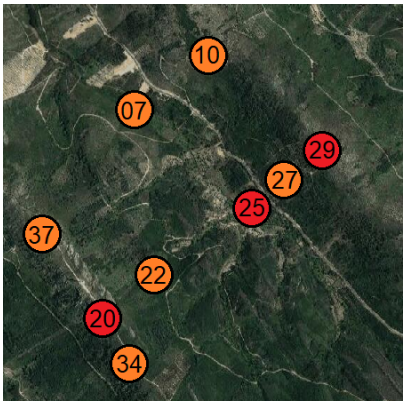

Figure 2. Position and tower numbers of the meteorological masts in Perdigão.

The data availability from January 2017 to June 2018 for mast 29 can be seen in Figure 3, where the white colour indicates missing data.

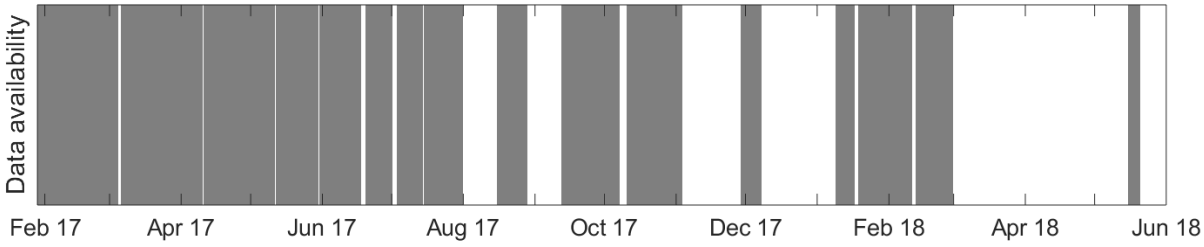

Figure 3. The data availability for mast 29 during the measurement period. Grey shows available data, and white shows missing data.

3. The Larsen model

This section contains a brief description of the Larsen extreme wind load condition model. More details about the Larsen model and parameter estimations may be found in [1]. Detailed descriptions the theoretical background and derivations of the model expression are given in [5, 8, 6]. A Python code with an implementation of the model can be found at the following GitLab repository: `https://gitlab.windenergy.dtu.dk/astah/Calibration_of_IEC_extremes`

3.1. Theory

The basis behind the Larsen model is an asymptotic expression for the distribution of the large wind velocity fluctuations for a given recurrence period. This approach combines a carefully selected transformation of relevant turbulence stochastic processes with earlier asymptotic extreme derivations done by Cartwright and Longuet-Higgens [7], where wind velocity excursion are assumed to be *Gaussian-distributed*. The first step in the Larsen derivation is to assume that the extreme wind velocity fluctuations (u_e) follow a *Gamma distribution* with a shape parameter of 1/2,

$$f\Big(u_e(z);\sigma_u(z),C(z)\Big) = \frac{1}{2\sqrt{2\pi C(z)\sigma_u(z)|u_e(z)|}}\exp\left(\frac{-|u_e(z)|}{2C(z)\sigma_u(z)}\right), \tag{1}$$

where $\sigma_u(z)$ is the standard deviation of the total data population at altitude z, and $C(z)$ is a height- and terrain-dependent dimensionless constant. The parameter $C(z)$, may be estimated by fitting eq.1 to the tail of a distribution of normalized wind velocity excursions:

$$u_e(t,z) = \frac{u(t,z)-\bar{U}(z)}{\bar{U}(z)}, \tag{2}$$

where $u(t,z)$ is the fluctuating wind velocity and $\bar{U}(z)$ is the ten-minute average wind speed. By applying a monotonic transformation to u_e (eq. 1) and normalizing with σ_u, the transformed variable ($\zeta_m = u_e/\sigma_u$) may be expressed by a Gumbel distribution. This distribution gives the asymptotic expression of u_e with any desired return period T. The *mode* of the Gumbel distribution (i.e. the most likely extreme) is given by

$$M[\zeta_m] = 2C(z)\ln(\kappa T). \tag{3}$$

Here κ gives the expected rate of local extremes and is expressed as

$$\kappa \equiv e^{-1/C(z)}\sqrt{\frac{m_2^3}{m_0^2 m_4}} \tag{4}$$

where m_0 is the zeroth-order spectral moment, or the variance, and m_2 and m_4 are the second- and the fourth-order spectral moments respectively. These spectral moments may be evaluated on closed form assuming the Kaimal spectrum (see Appendix A). Here we use the the Kaimal spectral model, as it is expressed in the IEC standard,

$$S_i(f) = 4\sigma_i^2 \frac{L_i}{\bar{U}} \left(1 + \frac{6fL_i}{\bar{U}}\right)^{-5/3} \tag{5}$$

where the subscript i refers to either the $u-$ or the v-component of the wind velocity and L is the length scale of turbulence.

The extremes defined/specified in the IEC code represent large gusts that are assumed to be coherent across the wind turbine rotor, which is an abstraction. This assumption may be approximated within the model framework by defining a cut-off frequency as

$$f_c = \frac{\bar{U}}{2D_R} \tag{6}$$

where D_R is the rotor diameter considered in the model application. By choosing a fluctuation 'spatial size' of twice the rotor diameter the turbulent excursions may be assumed approximately coherent across the rotor.

The wind velocity variance (m_0 in eq. A.1) and the other spectral moments are influenced by the introduced low-pass filter, where the variance becomes

$$\sigma_{if}^2 = \int_0^{f_c} S_i(f)df = \sigma_i^2 \left[1 - \left(1 + 6f_c \frac{L_i}{\bar{U}}\right)^{-2/3}\right]. \tag{7}$$

The reason for applying this cut-off frequency in the evaluation of spectral moments is to filter out the small-scale fluctuations of the wind field, or the high frequencies of the Kaimal spectrum. With this choice of f_c the model outputs become *rotor size dependent.*

3.2. Parameter estimation

The model theory and predictions can be applied with a few additional formulations that are provided in the IEC standard. We can apply the normal turbulence model (NTM) for the turbulence standard deviation,

$$\sigma_u = I_{\text{ref}} \left(\frac{3}{4}\bar{U} + b\right) \tag{8}$$

where I_{ref} is the reference turbulence intensity. It should be noted that by setting $b = 5.6$ m/s, σ_u represents the 90th percentile of the standard deviation as function of wind speed. The average standard deviation may be approximated by setting $b = 3.8$ m/s [2, p. 26].

For the vertical shear estimation we additionally need the coherence model

$$Coh(D, \bar{U}, f) = \exp\left(-12\sqrt{\left(\frac{fD}{\bar{U}}\right)^2 + 0.12\left(\frac{D}{L_u}\right)^2}\right) \tag{9}$$

which is a function of frequency f, mean wind speed $\bar{U}$ and the vertical distance D (the rotor diameter), or the spatial extent of the estimated shear event.

We will estimate the terrain- and height-dependent parameter $C(z)$ directly from measurements. It is however possible to use the prescribed equation from [1] for the parameter

$$C(z) = az + b \tag{10}$$

where a and b are constants that depend on the terrain type. The constants have been estimated for offshore/coastal ($a = 0.0013$, $b = 0.3026$), flat/homogeneous ($a = 0.0003$, $b = 0.3011$) and hilly terrain ($a = 0.0009$, $b = 0.3581$).

The ratio $\sigma_v/\sigma_u = 0.8$ may also adapted from the IEC standard, though in the current analysis this ratio is estimated from the measurements. This is because the IEC value refers to flat and homogeneous terrain, which is contrary to the terrain conditions at the investigated site. Finally, the Kaimal turbulence length scale is given in the IEC standard as, $L_u = 340$ m, $L_v = 113$ m (for heights above 60 m). We adapt this formulation in the current analysis as well as estimates directly from measurements.

3.3. EOG

The gust amplitude of the EOG load case may be estimated within the model framework by multiplying eq. 3 with the filtered standard deviation eq. 7 of the u-component of the wind velocity

$$M[u] = 2C(z)\sigma_{uf}\ln(\kappa T). \tag{11}$$

3.4. ECD

In the Larsen model the ECD load case is considered as joint extremes of turbulent dictated u-component and v-component wind velocity fluctuations. The derivation of the joint maxima can be found in [6], where the mode of the u-component extreme is

$$M[u_j] = 2C(z)\sigma_{uf}\ln\left(T\frac{m_{v4}m_{u2}}{m_{u0}m_{v2}}\right) \tag{12}$$

and the mode of the v-component extreme is

$$M[v_j] = 2C(z)\sigma_{vf}\ln\left(T\frac{m_{u4}m_{v2}}{m_{v0}m_{u2}}\right). \tag{13}$$

The total amplitude of the ECD gust may be calculated as

$$V_{cg} = \sqrt{M[u_j]^2 + M[v_j]^2} \tag{14}$$

and the associated direction change during these joint extreme becomes

$$M[\theta] = \tan^{-1}\left(\frac{M[v_j]}{\bar{U} \pm M[u_j]}\right) \tag{15}$$

3.5. EDC

The extreme direction change is defined here as an extreme wind velocity v-component excursion, with a zero u-component excursion,

$$M[v] = 2C(z)\sigma_{vf}\ln(\kappa T) \tag{16}$$

Based on this extreme v-component excursion, the direction change is calculated by

$$M[\theta] = \tan^{-1}\left(\frac{M[v]}{\bar{U}}\right) \tag{17}$$

3.6. EWS

Details of the derivation is available in [5] which, besides estimates of extreme short-term wind shears, also offer an estimate of the *most likely* spatial shape of the extreme shear excursion. Referring to [5] the extreme short-term wind shear excursion is defined by

$$M[\delta u] = 2C(z)\sigma_{\text{eff}} \ln(\kappa T) \tag{18}$$

where σ_{eff} is the effective standard deviation defined as

$$\sigma_{\text{eff}}^2 = 2(1-\rho)\sigma_{uf}^2. \tag{19}$$

Here ρ is the correlation coefficient estimated across a distance D. The formulation of the correlation coefficient may be found in Appendix B.

3.7. Return period function

The return period T is defined for the model implementation as function of wind speed. Here we use 50-years with the unit of seconds, (i.e $t = 50 \cdot 365 \cdot 24 \cdot 60 \cdot 60$ s). By multiplying t with the wind speed distribution $f(\bar{U})$ we obtain a wind speed dependent return period:

$$T(\bar{U}) = t \cdot f(\bar{U}) \tag{20}$$

$T(\bar{U})$ gives the time span within a particular wind speed bin during the defined return period. In order to have wind speed dependent model estimates we use $T(\bar{U})$ as input for the extreme predictions given in equations 11, 12, 13, 16 and 18.

3.8. Gust rise-time factor

The last relevant and important consideration of the Larsen model is the gust rise-time factor. This factor is introduced in the model as the extreme value predictions are not bound to any specific rise time. However, the gusts prescribed in the IEC standard all have specific rise times, and therefore we define the gust rise-time factor as a function of a predefined time-span,

$$f_{gr}\left(\tau_g, \frac{L_i}{\bar{U}}\right) = 1 - \frac{R(\tau_g, \frac{L_i}{\bar{U}})}{R(0)} \tag{21}$$

where $R(\tau_g, \frac{L_i}{\bar{U}})$ is the autocovariance as function of the time lag τ_g, or gust rise time. The autocovariance may be estimated with the inverse Fourier transform of the Kaimal spectrum, where the complete formulation of $f_{gr}\left(\tau_g, \frac{L_i}{\bar{U}}\right)$ is found in Appendix C. The gust rise-time factor is multiplied with all the model excursion (eqs. 11–13, 16 and 18) to achieve the desired gust rise time.

4. Basis for comparison

Before comparing the Larsen model extreme predictions to the Perdigão measurements it is important to process the measurements using some of the same assumptions that are used in the model description. To get a meaningful basis of comparison, the measurements are low-pass filtered with the same cut-off frequency as used in the estimation of the spectral moments in the Larsen model. Here we apply a second order Butterworth filter to each ten minute sample of the measurements with a cut-off frequency as defined in eq. 6.

Figure 4 shows an example of u-component wind velocity measurements that have been low-pass filtered. It may be seen how the small fluctuations, or high frequencies are removed from the filtered signal. These small fluctuations will therefore not influence the estimated extreme

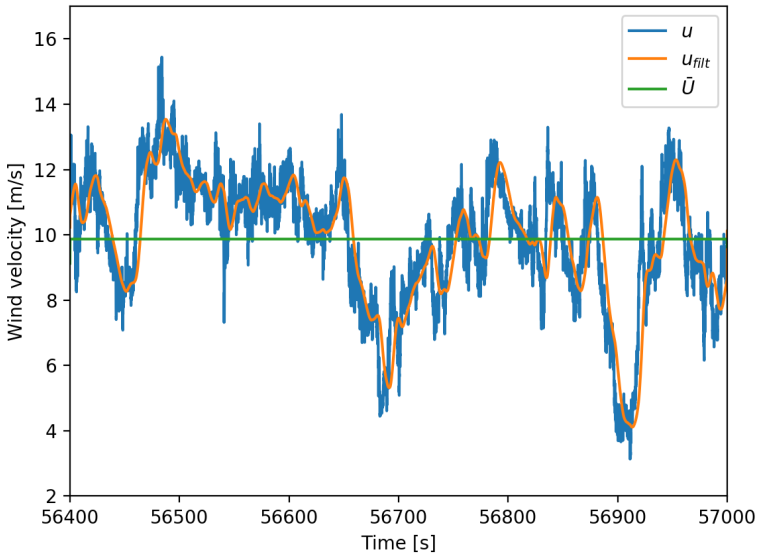

Figure 4. The longitudinal component of wind velocity measurements from 100 m in Perdigão. The measurements shown are: raw (blue), low-pass filtered (orange), and 10 minute mean (green).

statistics of the turbulent fluctuations. The applied low-pass filtering introduces a phase shift in the signal of approximately 2 seconds.

In this study we use the low-pass filtered measurements to estimate extreme values. For each 10-minute sample we subtract the same sample that has been shifted by the corresponding rise time and find the maximum value. The ECD is a special case though, as it is considered as a joint event of u-component and v-component extremes. In this case the index of maximum of the joint event is found by

$$ECD_{idx} = \max\left(\frac{U_f(t+\Delta t) - U_f(t)}{\max(U_f(t+\Delta t) - U_f(t))} \cdot \frac{|V_f(t+\Delta t) - V_f(t)|}{\max(|V_f(t+\Delta t) - V_f(t)|)}\right) \tag{22}$$

where U_f and V_f are respectively the u- and v-component of the filtered wind speed signal. The rise times for the different load cases are chosen according to the IEC standard which are: 3 s for the EOG, 6 s for the EWS and EDC, and 10 s for the ECD. These same rise times are also used in the Larsen model rise-time factor (eq. 21). These values are then finally extrapolated to give a 50-year return period contour with the IFORM (see next section).

5. Environmental contour method/ inverse FORM

The IFORM is a widely used method within wind energy to estimate the 50-year return period contour of a joint probability distribution, e.g of turbulence standard deviation (σ) and 10-minute mean wind speed ($\bar{U}$). More information on the IFORM may be found in e.g. [12], [11] and [13].

According to the IEC standard [3] the 10-minute mean wind speed is assumed to follow a Weibull distribution, and the 10-minute standard deviation of turbulent stream-wise velocity component fluctuations (σ_u) is assumed to follow either a log-normal- or a Weibull distribution conditional on mean wind speed (which is a new option ed.4 [3]). In this study we follow the

assumption of Weibull distributed wind speed and turbulence, and assume further that all the estimated wind velocity extremes, e.g. Δu_{3s}, follow Weibull distribution conditional on mean wind speed.

In IFORM analysis we need to obtain a "reliability index" β, which has its name from traditional FORM. The reliability index translates the desired return period T_r (here 50-years) into a measure in standard Gaussian space,

$$\beta = \Phi^{-1}\left(1 - \frac{T_t}{T_r}\right) \longrightarrow \Phi^{-1}\left(1 - \frac{1}{50n_m}\right) \tag{23}$$

where Φ^{-1} is the inverse Gaussian cumulative distribution function (CDF), T_t is the duration (here 10 minutes) of the period we measure each extreme within, and n_m is the number of 10-minute measurements we record over a one-year period. The length of the reliability index β may be estimated with

$$\beta = \sqrt{u_1^2 + u_2^2} \tag{24}$$

where u_1 and u_2 are the coordinates of a contour in standard Gaussian space. These coordinates may be transformed to the physical variable space of the current analysis using the Rosenblatt transformation [14]:

$$\bar{U} = F_{\bar{U}}^{-1}\Big(\Phi(u_1)\Big) \quad , \quad \Delta u = F_{\Delta u|\bar{U}}^{-1}\Big(\Phi(u_2)\Big) \tag{25}$$

where $F_{\bar{U}}$ is the Weibull CDF for the 10-minute mean wind speed, and $F_{\Delta u|U}$ is the conditional Weibull CDF for Δu:

$$F_V(V) = 1 - e^{(\bar{U}/A)^k} \tag{26}$$

$$F_{\Delta u|\bar{U}}(\Delta u) = 1 - e^{(\Delta u/A(\bar{U}))^{k(\bar{U})}} \tag{27}$$

Here k and A are respectively the shape and scale parameters of the Weibull distribution, and $k(\bar{U})$ and $A(\bar{U})$ are respectively the shape and scale parameters of the conditional Weibull distribution.

An important step in the current analysis is to estimate the shape parameter $k(\bar{U})$ and the scale parameter $A(\bar{U})$ as function of mean wind speed from the measurements.

6. The C(z) parameter at Perdigão

The wind velocity excursions (eq. 2) were calculated at 20 m, 60 m and 100 m height at Perdigão. Figure 5 shows the distribution of the excursions at 100 m height with a Gaussian fit to the distribution and the Gamma function (eq. 1) fit to the tail.

In this example the tail is defined as excursions beyond 5 times the standard deviation of the data distribution, which is 0.13 m/s at 100 m, 0.14 m/s at 60 m and 0.22 m/s at 20 m. It may be seen how the tail of Gamma distribution resembles a straight line on the semi-log plot. Though the straight line does not follow the data distribution in the whole tail range it does so at the tail edges, which are responsible for the extreme excursions.

The fitting of eq. 2 to the tails of the data distributions gave the following parameter estimates: C(100m) = 0.49, C(60m) = 0.48, and C(20m) = 0.43. These parameter estimates are used in the following section for the Larsen model.

7. Length-scale dependence

It may be seen from eqs. 11–13, 16 and 18 that the model excursions have a linear dependence on the 10-minute standard deviation, σ_i. However, it is not as intuitive to see the dependence of the Kaimal turbulence length scale on the modeled extremes. This is mainly due to the fact

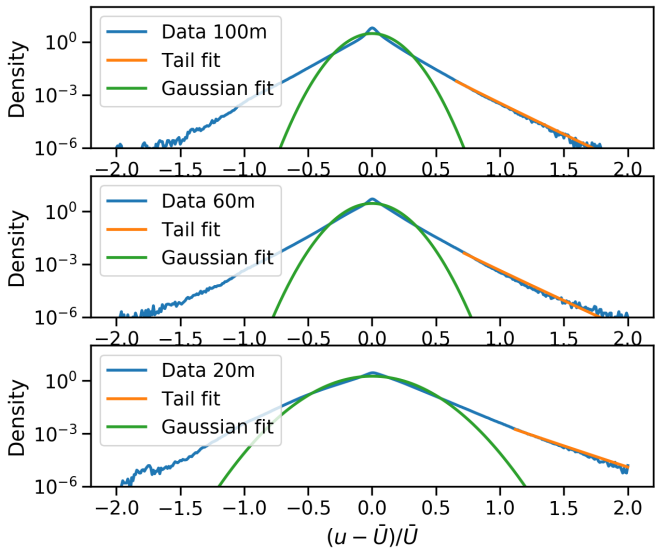

Figure 5. Wind velocity excursions (u-component) from linearly detrended measurement.

that the length scale enters both in the extreme amplitude estimates (eq. 11) and in the gust rise-time factor (eq. 21). Figure 6 shows the length scale-dependence of the product of the EOG excursion and the gust rise time factor with τ= 3 s at three different wind speeds. It is seen how the modelled EOG amplitude decreases with increasing length scale.

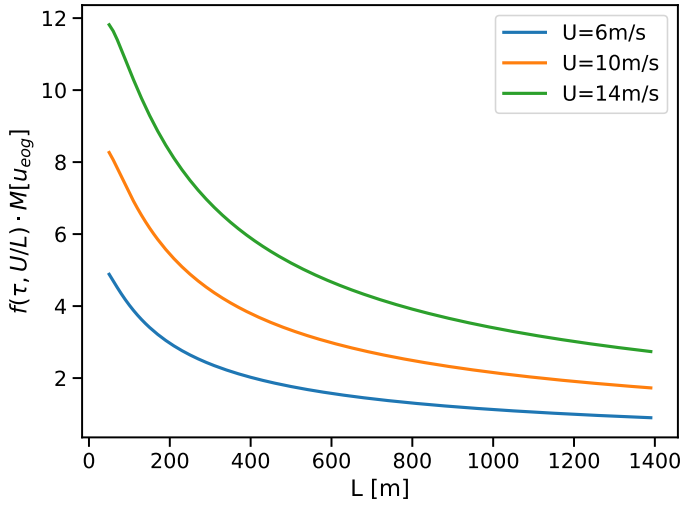

Figure 6. The product of the gust rise-time factor and the EOG excursion as function of the Kaimal turbulence length scale at three different wind speeds.

8. Comparison of IFORM analysis and Larsen model outputs

In the following section we compare the outputs of the Larsen model with the results from the IFORM analysis. One of the input parameters to the model is $I_{\text{ref}} = 0.16$, which has been

estimated according to the IEC standard from the measured 10-minute standard deviations (linearly detrended) from Perdigão.

Other general parameters include: D = 80 m for the EWS case and D = 100 m for the rest of the cases (corresponding to a medium-size rotor diameter). The 80 m choice for the EWS case is because the measured (extreme) shears are determined combining measurements performed at 20 m and 100 m heights, respectively. The measurements have been low-pass filtered with a cut-off frequency $f_c = \bar{U}/(2D_R)$ except for the EWS case where they are filtered with $f_c = \bar{U}/(D_R)$. The terrain and hight dependent parameter $C(z)$ is $C(100) = 0.49$ for all load cases except for the EWS, where we use $C(60) = 0.48$. The latter choice is because 60 m is the average altitude for the shear analysis. The ratio $\sigma_v/\sigma_u = 0.96$ has been estimated from the detrended measurements.

We tested the model with two different setups. In the first setup we used the Kaimal turbulence length scale, $L_u = 340$ m, $L_v = 113$ m adapted from the IEC standard with the 90th percentile 10-minute standard deviation (eq. 8 with b=5.6). For the second model setup we used the average 10-minute standard deviation (eq. 8 with b=3.8) and the Kaimal turbulence length scale estimated from the high frequency measurements at 100 m. The turbulence length scale was estimated by fitting eq. 5 to the power spectrum of 30-minute samples of wind speed measurements. The average of the estimated length scales was found to be $L_u = 135$ m and $L_v = 112$ m, which reflects the complex nature of the investigated site. See table 8 for the differences in the model setup.

Table 1. Model setup differences.

Setup 1	Setup 2
$L_u = 340$ m	$L_u = 135$ m
$L_v = 113$ m	$L_v = 112$ m
$\sigma_u = I_{\text{ref}}\left(\frac{3}{4}\bar{U} + 5.6\right)$	$\sigma_u = I_{\text{ref}}\left(\frac{3}{4}\bar{U} + 3.8\right)$

We have calculated the mean absolute percentage error (MAPE) between the model estimates and the corresponding points on the IFORM curves at discrete mean wind speeds $\bar{U}$ = [4,5,...,14,15] m/s:

$$MAPE = \frac{100\%}{n}\sum_{i=1}^{n}\left|\frac{A_i - F_i}{A_i}\right| \tag{28}$$

where A_i are points from the IFORM curve, and F_i are Larsen model outputs.

For the comparison a lower threshold was applied to the mean wind speed, and the extremes estimated from the measurements. It is worth mentioning, that this is consistent with the asymptotic character of the Larsen model with focus on large extremes. The thresholds are: 3.5 m/s on the wind speed, 1 m/s on the EOG and EDC extremes, 3 m/s on the EWS and 15° on the EDC. Because these thresholds were applied, we used the 3-parameter Weibull distribution fit to the 10-minute wind speed and all estimated extreme values. The location parameter of the Weibull distribution equals the threshold applied to the data.

8.1. EOG comparison

The Weibull parameters have been estimated as function of wind speed for the IFORM analysis. This is done by binning the extreme estimates Δu_{3s} and fitting the 3-parameter

Weibull distribution to each bin. To estimate the conditional parameters, a second order polynomial is fit to the $A(\bar{U})$ and $k(\bar{U})$ parameters. Thus, the estimated parameters are: $A(\bar{U}) = 1.3 \cdot 10^{-2}\bar{U}^2 - 0.12\bar{U} + 0.39$ and $k(\bar{U}) = 9.2 \cdot 10^{-3}\bar{U}^2 - 0.11\bar{U} + 1.2$. For the 10-minute mean wind speed the estimated Weibull parameters are: k = 2.8, A = 6.4 m/s.

In Figure 7 the estimated Δu_{3s} as function of wind speed are shown with blue dots. The output from the IFORM analysis is shown with an orange curve, and the Larsen model outputs with a green and a purple curve. The Larsen model setup 2 curve gives the highest estimates in the whole range.

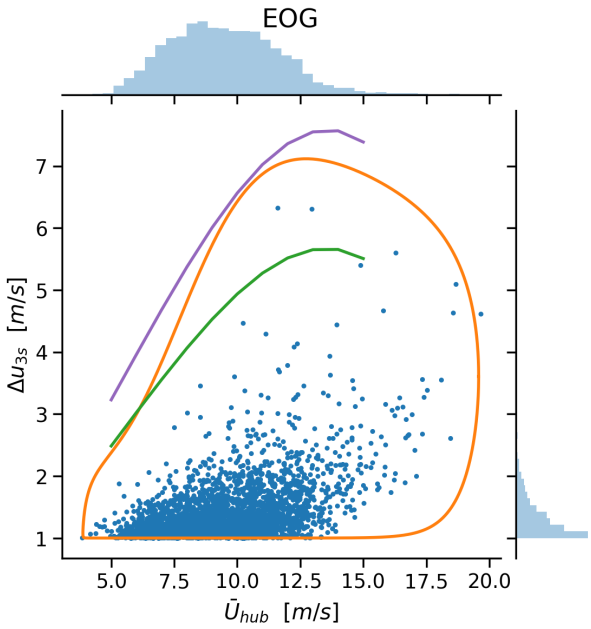

Figure 7. 3-second wind velocity extremes estimated from low-pass filtered measurements (blue dots). 50-year return period curves estimated with IFORM (orange), the Larsen model setup 1 (green) and Larsen model setup 2 (purple).

The $MAPE$ between the IFORM and Larsen setup 1 curves is: 16.2%
The $MAPE$ between the IFORM and Larsen setup 2 curves is: 12.4%

8.2. ECD comparison

Figure 8 and Figure 9 show the joint event of u-component and v-component, respectively. The extremes have been estimated with eq. 22. The estimated extremes are shown with blue dots, the IFORM estimated 50-year return period curve with orange and the Larsen model outputs with green and purple curves. It is seen that the Larsen model predicts lower values in the whole wind speed range for the u-component extremes, except for model setup 2 for wind speeds between 12 and 14 m/s. The Larsen model setup 1 predicts the highest values for the v-component extremes for wind speed bins 8 m/s - 15m/s.

The estimated conditional Weibull parameters for the u-component are: $A(\bar{U}) = 1.8{\cdot}10^{-2}\bar{U}^2 - 0.11\bar{U} + 0.72$ and $k(\bar{U}) = 4.9 \cdot 10^{-3}\bar{U}^2 - 2.0 \cdot 10^{-2}\bar{U} + 1.0$
The estimated conditional Weibull parameters for the v-component are: $A(\bar{U}) = 1.8 \cdot 10^{-2}\bar{U}^2 - 0.16\bar{U} + 0.93$ and $k(\bar{U}) = 0.011\bar{U}^2 - 0.14\bar{U} + 1.5$

For the 10-minute mean wind speed the estimated Weibull parameters are: k = 2.1, A = 5.0 m/s.

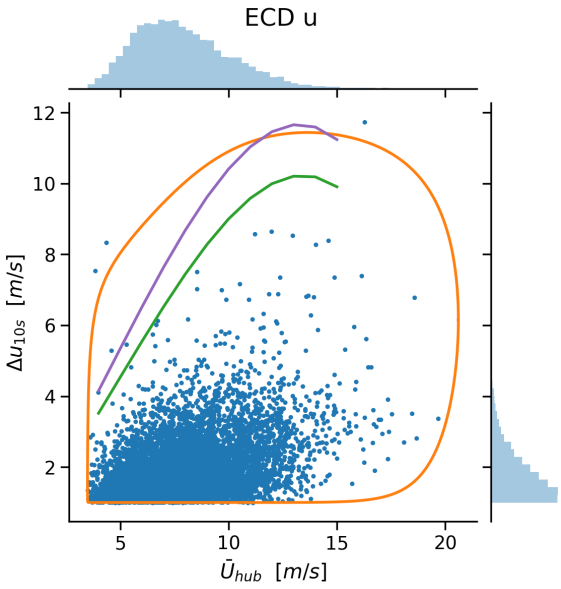

Figure 8. 10-second u-component wind velocity extremes estimated from low-pass filtered measurements (blue dots). 50-year return period curves estimated with IFORM (orange), the Larsen model setup 1 (green) and Larsen model setup 2 (purple).

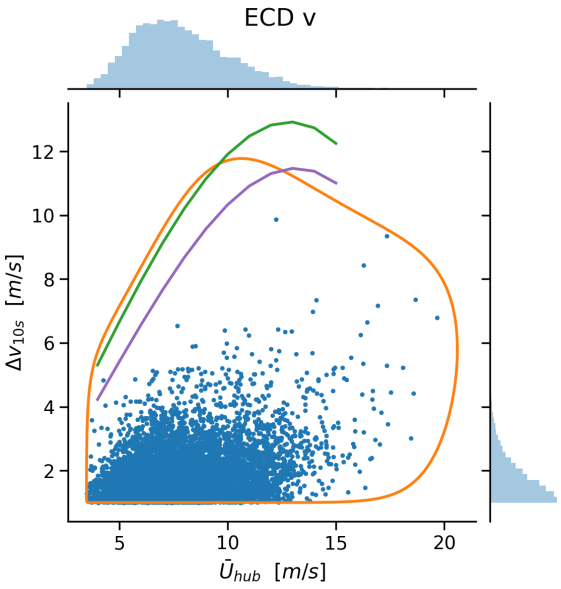

Figure 9. 10-second v-component wind velocity extremes estimated from low-pass filtered measurements (blue dots). 50-year return period curves estimated with IFORM (orange), the Larsen model setup 1 (green) and Larsen model setup 2 (purple).

u-component curves:
The $MAPE$ between the IFORM and Larsen setup 1 curves is: 23.8%.
The $MAPE$ between the IFORM and Larsen setup 2 curves is: 12.6%.
v-component curves:
The $MAPE$ between the IFORM and Larsen setup 1 curves is: 8.1%.
The $MAPE$ between the IFORM and Larsen setup 2 curves is: 13.3%.

8.3. EWS comparison

The extreme shear is estimated between 20 m and 100 m and here the measurements have been filtered with $f_c = \bar{U}/D$. The Larsen model predicts the stochastic part of the extreme shear only, and therefore we have added the mean background shear to the model predictions. This mean background shear is estimated from:

$$\bar{U}(z) = \bar{U}_{hub}(z/z_{hub})^{\alpha} \tag{29}$$

with $\alpha = 0.2$.

The estimated conditional Weibull parameters are: $A(\bar{U}) = 6.2 \cdot 10^{-2}\bar{U}^2 - 0.54\bar{U} + 1.75$ and $k(\bar{U}) = 1.5 \cdot 10^{-2}\bar{U}^2 - 9.9 \cdot 10^{-2}\bar{U} + 1.03$. For the 10-minute mean wind speed the estimated Weibull parameters are: k = 2.3, and A = 5.0 m/s. In Figure 10 the estimated extreme shear events are indicated with blue dots, the IFORM estimated shear curve with orange and the

Larsen model EWS estimates with green and purple curves. The Larsen model shows lower estimates in the whole wind speed range.

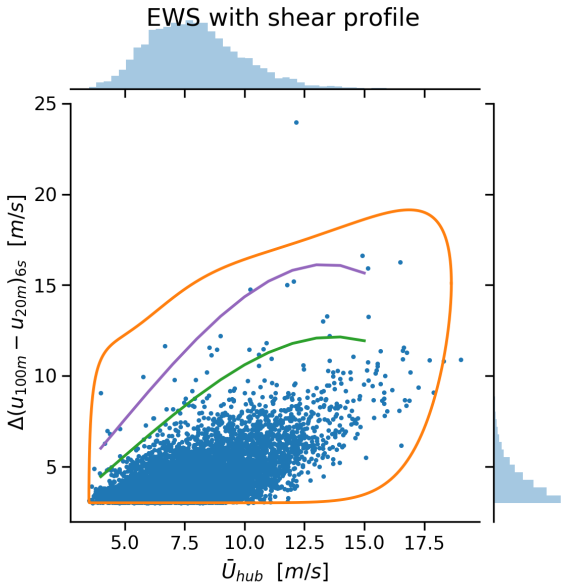

Figure 10. 6-second extreme wind velocity shear estimated from low-pass filtered measurements between 20 m and 100 m (blue dots). 50-year return period curves estimated with IFORM (orange), the Larsen model setup 1 (green) and Larsen model setup 2 (purple).

The $MAPE$ between the IFORM and Larsen setup 1 curves is: 40.8%.
The $MAPE$ between the IFORM and Larsen setup 2 curves is: 20.3%.

8.4. EDC comparison
In Figure 11 the estimated extreme 6-second direction change is shown with blue dots. The Larsen EDC model for both model setups is shown with a green and a purple curve. The Larsen model outputs underestimate the direction change in the whole wind speed range. Therefore, we also implemented the ECD model to predict the extreme direction change for comparison, which may be seen in Figure 12.

The estimated conditional Weibull parameters are: $A(\bar{U}) = 3.0 \cdot 10^{-2}\bar{U}^2 - 0.79\bar{U} + 10.2$ and $k(\bar{U}) = 2.8 \cdot 10^{-3}\bar{U}^2 - 3.5 \cdot 10^{-2}\bar{U} + 1.0$. For the 10-minute mean wind speed the estimated Weibull parameters are: k = 1.5 and A = 3.8 m/s.
EDC model curves:
The $MAPE$ between the IFORM and Larsen setup 1 curves is: 49.6%.
The $MAPE$ between the IFORM and Larsen setup 2 curves is: 54.4%.
ECD model curves:
The $MAPE$ between the IFORM and Larsen setup 1 curves is: 24.2%.
The $MAPE$ between the IFORM and Larsen setup 2 curves is: 21.7%.

9. Discussion
Comparing Figures 7–12 and the MAPE between the Larsen model and the IFORM analysis we observe the smallest differences for the EOG and the ECD load cases. The IFORM- and the

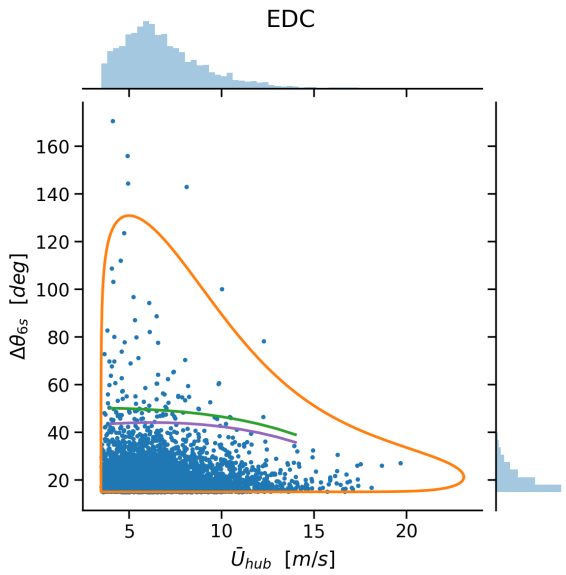

Figure 11. 6-second extremes wind direction change estimated from low-pass filtered measurements (blue dots). 50-year return period curves estimated with IFORM (orange), the EDC Larsen model setup 1 (green) and Larsen model setup 2 (purple).

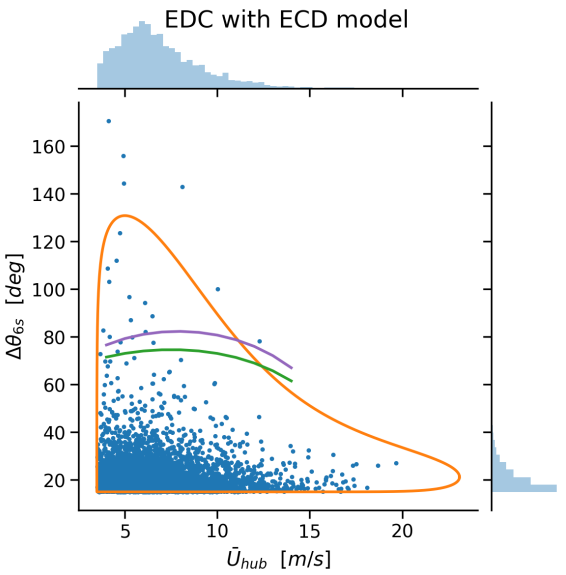

Figure 12. 6-second extremes wind direction change estimated from low-pass filtered measurements (blue dots). 50-year return period curves estimated with IFORM (orange), the ECD Larsen model setup 1 (green) and Larsen model setup 2 (purple).

Larsen model curves show somewhat different shapes, as the IFORM curves are estimated by fitting the Weibull distribution to the observed extreme data points, while the Larsen model only takes average values as input parameters. There are many possible factors that can contribute to these discrepancies, and we will discuss a few points here.

It is shown how the model output is sensitive to changes of the Kaimal turbulence length scale. It is seen in Figure 6 that the sensitivity to such changes is highest for the lower turbulence length scales, which is precisely in the range that we observe and implement.

The site specific estimate of L_u is 2.5 times lower than what given in the IEC standard. This is expected as our estimates are made in complex terrain, while the IEC prescription is for more flat and homogeneous terrain. The lateral component of the turbulence length scale is however approximately the same, and therefore the site specific ratio, $L_v/L_u = 0.83$, is much higher than what is given in the IEC standard. The Larsen model setup 2, results in higher extreme estimates for the model outputs, as lowering the turbulence length scale dominates the effects of lowering σ_u and/or σ_v. This is with two exception though: The v-component of the ECD and the EDC, because in these cases L_v is approximately the same, so the higher σ_v leads to the higher estimates for model setup 1.

We observe high extreme direction changes for low wind speeds that decrease with increasing mean wind speeds. This might relate to buoyancy effects associated with non-neutral stratification of the atmospheric boundary layer, which are known to be relatively more significant in the low wind speed regime. Being based on the observed extremes, the IFORM curve displays well this decrease, similar to how extreme direction change is modelled in the IEC standard. However, the Larsen EDC model does not predict this general shape and greatly underestimate the extreme direction change, especially in the low wind speed range. Higher direction changes are modelled by applying the ECD model to predict the direction change, but

this model still underestimates the direction change for wind speeds below 11 m/s.

The Larsen model output for the EWS showed lower estimates compared with the IFORM analysis. A likely explanation is that the IEC coherence model is relatively conservative (cf. [4]), thus in turn leading to a high correlation coefficient. It may be seen in eq. 19 that conservative coherence estimates lead to lower prediction of extreme shear excursion than if a lower non-conservative value of ρ is used.

A possible further development of the model could be to provide more terrain dependent options of the model input parameters. E.g. the Kaimal turbulence length scales (L_u and L_v) and different coherence models to estimate the correlation coefficient. This might lead to more realistic and more conservative model outputs.

It should be noted that the IFORM analysis does not provide 'true' 50-year return values, as this analysis is also based on assumptions. If e.g. the extreme distribution fits were based on a log-normal assumption, alternative to the chosen Weibull assumption, different extreme 50-year return period curves would result. It is seen from Figures 8 and 11 that there are some data points that fall outside the 50-year return period contour, although the number of data points roughly corresponds to one year. This indicates either measurement errors, or that the Weibull distribution underestimates the tails of the measured/estimated extreme values. It is also interesting to note, that for the majority of the IFORM Weibull fits, the shape parameters come close to one, and thus approach the assumed exponential character of the tails assumed in the Larsen model.

There are many different kinds of flow phenomena that may be expected in the complex terrain in Perdigão [9]. These may not be represented by a model that is based on homogeneous turbulence and neutral conditions. These phenomena can also show up as extreme values in data distributions, making it difficult to fit a theoretical distribution to the data.

10. Conclusion

In this paper we implement the Larsen model for the first time in complex terrain. The model outputs are compared with IFORM analysis made on a comprehensive data set, spanning the whole wind speed range. The comparison between them gives a MAPE in the range 8.1% and 65.8%. The IFORM and the Larsen model predictions give the most similar results for the EOG- and the ECD load cases. The EWS load case underestimated the extreme share in the whole wind speed range, but could potentially improve by using a more appropriate coherence model. The EDC load case does not predict the expected extreme direction change, and this load case requires new kind of modelling. The Larsen model should not be used for load- or site assessment on its own in the current state i.e. by using the IEC assumptions for input. However, with further validation, calibration and mapping of the input parameters, the Larsen model shows potential to provide very accurate extreme gusts predictions.

Appendix A.

The low-pass filtered spectral moments evaluated with the Kaimal spectrum are

$$m_0 = \sigma_i^2 \left[1 - \left(1 + 6f_c\frac{L_i}{\bar{U}}\right)^{-2/3}\right] \tag{A.1}$$

$$m_2 = \sigma_i^2 \frac{\bar{U}^2}{54L_i^2}\left[\frac{3}{4}\left(1 + 6f_c\frac{L_i}{\bar{U}}\right)^{4/3} - 6\left(1 + 6f_c\frac{L_i}{\bar{U}}\right)^{1/3} - \frac{3}{2}\left(1 + 6f_c\frac{L_i}{\bar{U}}\right)^{-2/3} + \frac{27}{4}\right] \tag{A.2}$$

$$m_4 = \sigma_i^2 \frac{\bar{U}^4}{1944L_i^4}\left[\frac{3}{10}\left(1 + 6f_c\frac{L_i}{\bar{U}}\right)^{10/3} - \frac{12}{7}\left(1 + 6f_c\frac{L_i}{\bar{U}}\right)^{7/3} + \frac{9}{2}\left(1 + 6f_c\frac{L_i}{\bar{U}}\right)^{4/3} - 12\left(1 + 6f_c\frac{L_i}{\bar{U}}\right)^{1/3} - \frac{3}{2}\left(1 + 6f_c\frac{L_i}{\bar{U}}\right)^{-2/3} + \frac{729}{70}\right] \tag{A.3}$$

where $\bar{U}$ is the 10-minute mean wind speed, L_i is turbulence length scale of the i'-component, and f_c is the cut-off frequency to apply in the model application.

Appendix B.

The correlation coefficient for EWS is determined as

$$\rho = \frac{1}{\sigma_{uf}^2}\int_0^{\bar{U}/D} Coh(D, \bar{U}, f)S(f)df \tag{B.1}$$

where $Coh(D, \bar{U}, f)$ is from eq. 9, and $S(f)$ is from eq. 5. By introducing the reduced frequency, $f_r = fD/\bar{U}$, the correlation coefficient integral is re-formulated as

$$\rho = \frac{4\sigma_u^2 L_u}{\sigma_{uf}^2 D}\int_0^1 \exp\left[-12\sqrt{f_r^2 + \left(0.12\frac{D}{L}\right)^2}\right]\left(1 + 6f_r\frac{L}{D}\right)^{-5/3} df_r \tag{B.2}$$

This integral has to be solved numerically to estimate ρ. It is seen that ρ is wind speed independent by expressing it using the reduced frequency. Previous analysis [4] has shown the IEC coherence to be larger than observed in measurements, therefore typically giving rise to larger than measured correlation coefficients and thus in turn too low efficient turbulence standard deviations.

Note that for the EWS load case, we consider a higher cut-off frequency for the low-pass filter than for the other load cases. Here we use $f_c = U/D_R$, when we estimate σ_{uf} as in eq. 7. This is done because the EWS load case is not assumed a coherent excursion across the rotor in the IEC standard. Rather it represents fluctuations of opposite sign across the rotor.

Appendix C.

When the autocovariance in eq. 21 is formulated with the inverse Fourier transform of the Kaimal spectrum, the gust rise-time factor becomes:

$$f_{gr}(\tau_g, \frac{L_i}{\bar{U}}) = 1 - \frac{2}{27\Gamma(\frac{5}{3})}\left(9\Gamma\left(\frac{2}{3}\right){}_1F_2\left(1; \frac{1}{6}, \frac{2}{3}; -\left(\frac{\pi\tau_g\bar{U}}{6L_i}\right)^2\right) + \left(3\pi^5\frac{\bar{U}^2}{L_i^2}\right)^{1/3}\tau_g^{2/3}\left[3\sin\left(\frac{\pi\bar{U}\tau_g}{3L_i}\right) - \sqrt{3}\cos\left(\frac{\pi\bar{U}\tau_g}{3L_i}\right)\right]\right). \tag{C.1}$$

Here $\Gamma()$ is the gamma function and ${}_1F_2()$ is the generalized hypergeometric function. The gust rise-time consideration is applied by multiplying the factor with the extreme excursions described in the paper. By applying the gust rise-time factor, only the largest fluctuations within a certain time-span are taken into consideration.

References

[1] Larsen, G. C. and Hansen, K. S.: Rational Calibration of Four IEC 61400-1 Extreme External Conditions. Wind Energy 11(6), 685702, 2008.
[2] IEC 61400–1, Edition 3, Wind turbine generator systems – Part 1: Safety requirements, International Electrotechnical Comission, Geneva, Switzerland, 2005.
[3] IEC 61400–1, Edition 4, Wind turbine generator systems – Part 1: Safety requirements, International Electrotechnical Comission, Geneva, Switzerland, 2019.
[4] Larsen, G. C. and Hansen, K. S.: Spatial coherence of the longitudinal turbulence component. Proceedings of EWEC 2003. Vol. CD-ROM. CD 2 Brussels : European Wind Energy Association (EWEA), 2003.
[5] Larsen, G. C. and Hansen, K. S.: Statistical Model of Extreme Shear. Journal of Solar Energy Engineering, Vol. 127, No. 4, 2005, p. 444-455.
[6] Larsen, G. C.: An asymptotic closed form solution for the distribution of combined wind speed and wind direction extremes. Journal of Physics: Conference Series (Online), Vol. 75, 2007, p. 20.
[7] Cartwright, D. E. and Longuet-Higgins, M. S.: The statistical distribution of the maxima of a random function. Proceedings of the Royal Society of London. Series A, Mathematical and Physical Sciences, 237(1209),212232, 1956.
[8] Larsen, G. C. and Hansen, K. S.: The statistical distribution of turbulence driven velocity extremes in the atmospheric boundary layerCartwright/Longuet-Higgins revised. EUROMECH colloquium 464b, Wind energy. International colloquium on fluid mechanics and mechanics of wind energy conversion, 111114, Oldenburg (DE). Springer-Verlag Berlin, 2006.
[9] Fernando, H. J. S., et al. The Perdigão: Peering into Microscale Details of Mountain Winds. Bulletin of the American Meteorological Society, May, 799819, 2019.
[10] Menke R. and Mann J. Perdigão 2017: Laser survey of measurement masts. DTU Wind Energy Report, DTU Wind Energy, 2017.
[11] Winterstein, S. R., Ude, T. C., Cornell, C. A., Bjerager, P., and Haver, S.: Environmental parameters for extreme response: inverse form with omission factors. In Proceedings of the 6th international conference on structural safety and reliability (ICOSSAR93), 551557, 1993.
[12] Saranyasoontorn, K. and Manuel, L: Design loads for wind turbines using the environmental contour method [15]. Journal of Solar Energy Engineering, 128:554, 2006
[13] Moon, J. S., Sahasakkul, W., Soni, M., and Manuel, L.: On the use of site data to define extreme turbulence conditions for wind turbine design [39]. Journal of Solar Energy Engineering, 136, 2014
[14] Rosenblatt, M.: Remarks on a multivariate transformation. The Annals of Mathematical Statistics, 23(3):470472, 1952.